X-ray-absorption spectroscopy studies of glassy As_2S_3: The role of rapid quenching

C. Y. Yang, D. E. Sayers, and M. A. Paesler
Department of Physics, North Carolina State University, P.O. Box 8202, Raleigh, North Carolina 27695-8202
(Received 6 March 1987)

We have examined the effect of the thermal quenching rate on the structure of As_2S_3 chalcogenide glasses. Structural differences among glasses are discussed on the basis of results of x-ray-absorption measurements. We find that small structural differences are seen among glassy As_2S_3 samples bulk quenched from various temperatures between 350 and 800 °C. Comparatively large changes are observed, however, among samples quenched from annealing temperatures between 200 and 300 °C with the structural disorder decreasing with increasing annealing temperature. Material quenched at 300 °C shows a strong tendency toward ordering. Structural differences among samples are discussed in terms of (1) distortions in the As—S—As bond angles between helices and within a helix and (2) deviations of the As apex angles.

I. INTRODUCTION

The structural, vibrational, electronic, and optical properties of chalcogenide glasses have been the object of much interest.[1] This interest is a manifestation of the fact that chalcogenide materials are of great technological importance and have many potential applications. However, in spite of much experimental and theoretical work, a number of unusual phenomena such as photostructural change[2] and thermostructural changes[3] are still not well understood. These phenomena are particularly manifest in the arsenic-sulfur system.

It is well known that physical properties of the As-S system are strongly dependent upon the preparation method and subsequent sample treatment. In particular, the optical gap of the As-S system depends sensitively on the thermal quenching rate and composition. For bulk glassy (*g*-) As_2S_3, the various reported values of the slope of the optical-absorption edge vary by as much as 25%,[4] and the reason is assumed to be due to differences in the quenching rate. Since the optical-absorption edge depends to a large extent on the details of sample preparation and subsequent annealing,[1] it has been suggested[4] that the temperature of the melt and the quench rate are presumably responsible, and that differences in them are reflected in varying degrees of disorder. The compositional dependence of the optical gap of the melt-quenched As_xS_{1-x} system has been investigated by Kosek *et al.*[5] Near stoichiometry (40 at. %) the optical gap drastically decreases with increasing As content. Since structural changes can strongly affect the optical and electrical properties of this system, lack of accurate knowledge about these changes may lead to the misinterpretation of experimental results. A careful investigation[6] of the effect of the thermal quenching rate and composition on the structure of As_xS_{1-x} chalcogenide glasses, therefore, is clearly of interest.

A great deal of work has been done to determine the structure of the As-S system using x-ray and neutron diffraction.[7–10] Many diffraction studies of As_xS_{1-x} glasses have placed great emphasis on the first sharp diffraction peak (FSDP) at low scattering vector Q, about 1.3 $Å^{-1}$. There has, however, been much controversy on the origin of the anomalous FSDP which has been discussed in terms of several models such as layers, chains, or large molecule clusters. Similar behavior is also observed in the temperature dependence of the x-ray diffraction pattern of vitreous silica.[11] Recently, Wright *et al.*[12] have discussed possible interpretations of the behavior of the FSDP. They concluded that the evidence for specific structural features such as layers in bulk chalcogenide glasses is much less certain.

Kawamura *et al.*[13,14] have reported a shift of low-frequency Raman scattering of As_2S_3 glass as a function of different quenching temperatures (from 170 to 400 °C) and as a function of annealing temperature (from 25 to 210 °C). They interpret both effects of quenching and annealing on the structure of the glass in terms of an "outrigger raft" model and propose that the ordering of the arrangement of the rafts becomes more random as the quenching temperature or annealing temperature is raised. These rafts, according to Phillips,[15] are associated with van der Waals forces operating between chalcogen atoms with lone pair electrons. However, there has also been controversy over the structural significance of the low-frequency Raman scattering. For example, Nemanich[16] has examined the low-temperature Raman spectra for the corresponding layerlike material, *g*-$GeSe_2$, and found no evidence of long-range layerlike correlation. It has been alternatively suggested that the low-frequency Raman scattering is dominated by either acoustic modes[17] or opticlike modes.[15] Hence, the low-frequency Raman feature could be either due to a combination of the boson occupation factor and matrix element variations[17] or due to the rigid-layer modes.[15]

We take another approach to studying structural changes in the As-S system by using x-ray-absorption spectroscopy (XAS). The XAS technique has become a powerful tool in probing the electronic properties and atomic structure of a wide range of materials.[18] The x-

ray-absorption spectrum can be divided into two regions: the x-ray-absorption near-edge structure (XANES), which typically ranges within 30 eV of the threshold, and the extended x-ray-absorption fine structure (EXAFS), which covers an energy range up to several hundred eV above the edge. The XANES contains information about the binding energies, coordination geometry, symmetry of the unoccupied electronic state, and effective atomic charge on the absorbing atom. The EXAFS provides useful information concerning the types and number of coordinating atoms and the corresponding interatomic distance and disorder of the shells.

The present paper is organized into four sections. In Sec. II we describe the experimental details relating to sample preparation and characterization and the x-ray-absorption measurements. In Sec. III we discuss the EXAFS technique and data analysis. In Sec. IV we present the result and discuss the effect of the quenching rate on the structure of g-As_2S_3.

II. EXPERIMENTAL

Small quantities of g-As_2S_3 were placed in quartz ampoules which were evacuated to 10^{-6} Torr and backfilled with argon before being sealed. Ampoules were heated at 650 °C in a rocking furnace for 24 hours, ice quenched, and then returned to room temperature. These ampoules were then reheated to temperatures ranging from 200–800 °C (call this T_Q) before being ice quenched and returned to room temperature a second time.

We annealed our samples for 2, 4, and 12 hours and saw no difference in any effects. Consequently, we felt that the annealing effect was saturated at 2 hours. There are also well-known differences between glassy and thin-film samples, but the present work concentrates on the bulk glasses. We leave the study of thin films to a later work.

The crystallinity of c-As_2S_3 samples was confirmed by x-ray diffraction using Cu $K\alpha$ radiation. Lattice parameters were matched with known crystalline spectra. Impurities were less than 0.2%, as determined by electron microscopy. It was confirmed by x-ray diffraction measurements that phase separation and crystallization had not occurred for the g-As_2S_3 samples.

Samples were separately ground to fine powders and placed on Kapton tape. About six to eight layers were used to make samples of sufficient thickness for the EXAFS measurements to be made. In order to avoid thickness effects (an important source of error in the measurement of the Debye-Waller term), various thicknesses were measured. All of the uniform samples used in this work had an edge step of $\Delta(\mu x) < 1.1$, which is lower than the theoretical optimum[19] so that the EXAFS does not change for different thicknesses.

The XAS spectra performed at the K edge of As were measured at the National Synchrotron Light Source on the X-11A beam line using a double-crystal monochromator with Si(111) crystals. The beam energy was 2.5 GeV and electron currents were typically 30–60 mA. The relative angle between the two monochromator crystals was adjusted to detune the incident beam by 20% in order to reduce the higher harmonic content of the beam. Three ionization chambers filled with appropriate gases were used to measure x-ray intensities, with the third chamber used to calibrate the position of the As K edge, using c-As as a standard. Transmission measurements on each sample were made at liquid-nitrogen and room temperatures. The data were consistent during several different runs.

III. THE EXAFS TECHNIQUE AND DATA ANALYSIS

Phenomenologically, the EXAFS is simply the oscillatory modulation of the x-ray-absorption photon energy beyond the absorption edge. In a transmission experiment the absorption data are obtained from

$$\mu x = \ln(I_0/I) , \tag{1}$$

where μ is the total absorption coefficient, I_0 is the incident of the monochromatic x-ray beam, I is the intensity of the beam which is transmitted through the sample, and x is the sample thickness. The measured x-ray absorption for g-As_2S_3 is shown in Fig. 1; EXAFS results from the interference between the outgoing photoelectron wave from the x-ray absorbing atom and the backscattered waves from surrounding atoms. This interference is sensitive to the amplitude and phase of the waves, i.e., to the number, the nature, and the distance of the surrounding atoms. By making a number of approximations,[20] structural information contained in the EXAFS interference function can be described as

$$X(k) = \frac{\mu - \mu_0}{\mu_0} = -\sum_i \frac{N_i}{kR_i^2} F_i(k) e^{-2R_i/\lambda} e^{-2\sigma_i^2 k^2} \sin[2kR_i + \phi_i(k)] , \tag{2}$$

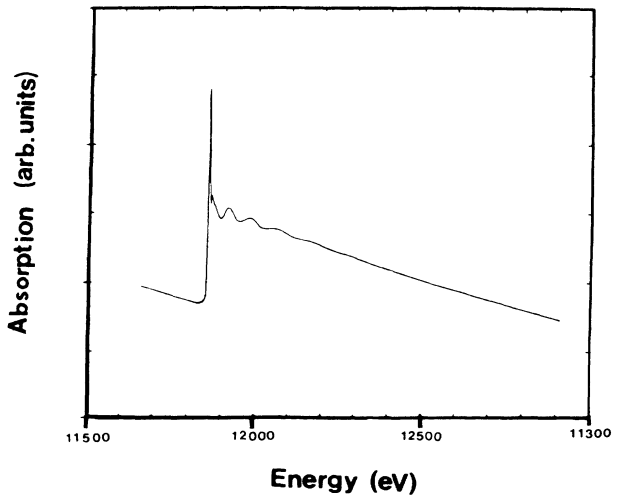

FIG. 1. x-ray absorption as a function of photon energy about the As K edge at 11.867 keV in g-As_2S_3 quenched at 300 °C.

where μ_0 is the smoothly varying background absorption, the sum is over the coordination shells at an average distance R_i from the absorbing atom, N_i is the number of scattering atoms in the ith shell at distance R_i, and λ is the electron mean free path. The electron wave vector is defined as $k=[(2m/\hbar^2)(E-E_0)]^{1/2}$, where E is the photon energy and E_0 and m are the threshold energy and mass of the electron, respectively. $F_i(k)$ is the magnitude of the backscattering and is a function of the type of scattering atom. $\phi_i(k)$ is a phase shift produced by the fact that the photoelectron moves in the potential of the central and backscattering atoms. σ_i^2 is the mean-square deviation from the average distance between the origin atom and scattering atom. The Debye-Waller factor σ^2 arises from both structural disorder and thermal motion of the atoms in a given shell so that

$$\sigma^2=\sigma_{\rm st}^2+\sigma^2(T) . \tag{3}$$

Structural disorder can be due either to a single site with different bond lengths or an ensemble of different sites. The structural disorder contribution to the Debye-Waller factor can be estimated by

$$\sigma_{\rm st}^2=\sum_{i=1}^{N}\frac{(r_i-r_0)^2}{N} , \tag{4}$$

where r_i-r_0 is the deviation from the mean-square distance r_0. For example, the structural disorder for the first As-S shell of c-As_2S_3 is 1.5×10^{-3} Å^2. In principle, static structural and thermal vibrational disorder can be separated by measuring the EXAFS at several temperatures.

The standard analysis of the data consists of three major stages: (a) extraction of the EXAFS signal from the raw data by removing the absorption background, (b) Fourier transformation of the normalized $\chi(k)$ to reveal the major frequency components and isolation of the single-shell data by Fourier filtering, and (c) determination of structural information from the filtered data. These steps include preedge subtraction, normalization, deglitching (if necessary), conversion to k space, removal of the atomic background, Fourier transformation, and filtering in r space. With the filtered single-shell data decomposed into phase and amplitude functions, if only a single type of scatterer is present, the ratio method[21] is usually used to extract structural parameters.

In the study of quenching effect on the structure of g-As_2S_3, the ratio method is applied to determine Debye-Waller factors by plotting the logarithm of the ratio of the first shell amplitude of the g-As_2S_3 sample and c-As_2S_3 as a standard versus k^2. The amplitudes of filtered data are determined as functions of k. From Eq. (2) the amplitude of this envelope function is determined by the number of neighbors N, the backscattering amplitude $F(k)$, and σ^2. Since the environments of As atoms are the same, i.e., same absorber-backscatterer pairs for both the samples and standard, and N and the function $F(k)$ are the same, any differences in the envelope function should be due to differences in σ^2. Figure 2 shows a comparison of the amplitude EXAFS function multiplied by k and of the filtered $k^3\chi(k)$ for the first shell of

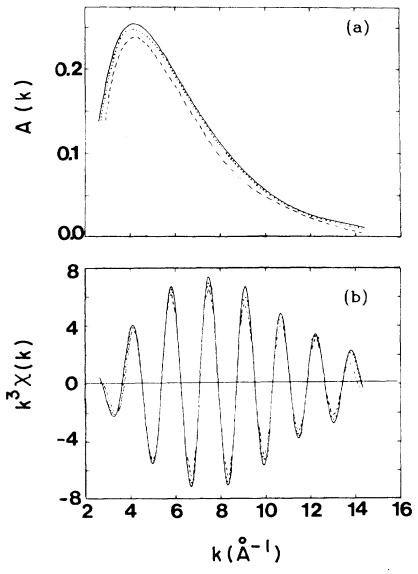

FIG. 2. (b) Fourier filtered $k^3\chi(k)$ of the first shell (a) normalized EXAFS amplitude function multiplied by k. Solid line, c-As_2S_3; dotted line, g-As_2S_3 quenched at 300 °C; dashed line, g-As_2S_3 quenched at 800 °C.

c-As_2S_3 and g-As_2S_3 quenched at 300 and 800 °C. To extract σ^2, we may take the ratio

$$\ln(\chi_g/\chi_c)=-2k^2(\sigma_g^2-\sigma_c^2) . \tag{5}$$

A plot of the logarithm of the ratio of the amplitude versus k^2 gives a straight line of slope equal to twice the difference in σ^2 and an intercept at $k=0$, as shown in Fig. 3. Note that in Fig. 3 straight lines are obtained. In the same way, information about the difference in the mean-square relative displacement (MSRD) $\sigma^2(T)$ between liquid-nitrogen temperature (LNT) and room tem-

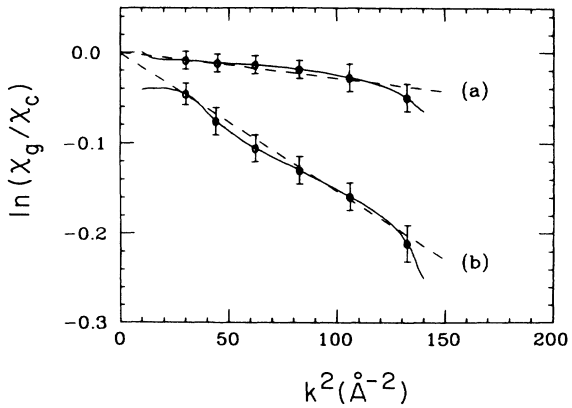

FIG. 3. Examples of the logarithm of amplitude ratio between two different g-As_2S_3 samples (a) quenched at 300 °C and (b) quenched at 800 °C. The data of c-As_2S_3 were used as a standard.

perature (RT) of each sample is also determined. In order to separate the contributions from relative structural disorder, σ_{st}^2, and thermal disorder, $\sigma^2(T)$, we must evaluate $\sigma^2(T)$ from theory. It has been theoretically and experimentally shown[22,23] that the Einstein model, in which only the bond stretching vibrational modes are considered,[24] is sufficient to account for the thermal vibrational contribution of $\sigma^2(T)$ for the first shell of EXAFS. The Einstein model for $\sigma^2(T)$ can be written in a simple form

$$\sigma^2(T)=\frac{\hbar}{2\mu\omega_E}\coth\left[\frac{\hbar\omega_E}{2k_BT}\right], \quad (6)$$

where μ is the reduced mass, ω_E is the Einstein frequency, k_B is the Boltzmann constant, and T is the temperature. The difference between $\sigma^2(T)$ measured at two temperatures, T_1 and T_2, is therefore

$$\Delta\sigma^2(T)=\frac{h^2}{2\mu k_B\Theta_E}\left[\coth\left[\frac{\Theta_E}{2T_1}\right]-\coth\left[\frac{\Theta_E}{2T_2}\right]\right], \quad (7)$$

where $\Theta_E=\hbar\omega_E/k_B$ is the Einstein temperature, $\Delta\sigma^2(T)$ is in units of Å^2, and, for our results, T_1 is liquid-nitrogen temperature and T_2 is room temperature. Table I lists the experimental $\Delta\sigma^2(T)$ values and values of $\Delta\sigma^2(T)$, σ^2(LNT), and σ^2(RT) that are calculated from an Einstein model, using the Θ_E values indicated.

IV. RESULTS AND DISCUSSION

Since glassy alloys are usually obtained by rapid quenching of melts, the glassy state is generally considered to be the frozen liquid state. During rapid quenching, the atoms are frozen into a metastable state, not only with respect to the c state, but also with respect to a well-relaxed glassy state. Therefore, in contrast to crystalline materials or liquids which exist in unique equilibrium states, many metastable states, depending on preparation method and later treatment, may exist in glasses. In this study, the fundamental questions concerning the glassy state structure arising from variations in the method of preparing samples are (1) to what extent are their structures similar to a well-relaxed, more stable g state, and (2) to what extent do they show ordering resembling that which may be found in crystal?

The $\chi(k)$ data multiplied by k^3 and the corresponding magnitude of the Fourier transform of $k^3\chi(k)$ over a k range of 2.6–15.8 Å^{-1} are shown in Fig. 4 for c-As_2S_3 and g-As_2S_3 quenched at 300 and 800 °C. Differences can be seen in the amplitude of Fourier transform of the first peak. Other changes in the second shell structure are also seen in g samples. In the first shell of the isolated EXAFS, the ratio method shows that the short-range order (SRO) of the crystal is preserved in g-As_2S_3. In other words, the first neighbor distance, $R_{\text{As-S}}=2.28$ Å, and coordination number, $N_{\text{As-S}}=3$, are the same. The differences between c- and g-As_2S_3 samples are only due to differences in $\Delta\sigma^2=\sigma^2$ (crystal) $-\sigma^2$ (glass). This relative structural disorder, $\Delta\sigma^2$, arises mainly from structural disorder, because the thermal vibrational disorder of c- and g-As_2S_3 samples are the same[25] within the error. The contribution of thermal disorder to the Debye-Waller factor in the first shell of all samples has been listed in Table I.

A plot of the relative structural disorder versus the quenching temperature T_Q is shown in Fig. 5. Above the melting temperature, $T_M=310\pm5$ °C,[26] the disorder increases with increasing T_Q. Thus rapid cooling of liquid As_2S_3 at a high temperature produces a more disordered structure in g samples because the atoms have insufficient time to relax from the high-temperature atomic configuration to the low-temperature atomic configuration. Therefore this change in the relative structural disorder values should not be considered an anomalous phenomenon. Such a behavior is connected with the changes of structural SRO and compositional SRO. Recently, based on Raman scattering spectra, Tanaka *et al.*[27] have suggested that As—As and S—S homopolar bonds (wrong bonds) and As—S heteropolar bonds are chemically mixed in As_2S_3 glasses quenched at various temperatures between 350 and 1100 °C. It is, therefore, assumed that an enhancement of the compositional disorder which results in the shift of the band gap toward lower energy occurs at higher quenching temperature. The approximately 1% homopolar bonds[27] that are contained in the As_2S_3 glass quenched above the melting temperature are below detectable limits for EXAFS measurements. The increased relative structural disorder with increasing quenching temperature observed by EXAFS may be due to chemical disorder

TABLE I. Values of Θ_E calculated from an Einstein model fit and experimental σ^2 and Einstein σ^2 for g-As_2S_3 samples at different quenching temperatures T_Q.

Sample T_Q (°C)	Θ_E (K)	$\Delta\sigma^2_{\text{expt}}$ (10^{-4} Å^2)	$\Delta\sigma^2_{\text{calc}}$ (10^{-4} Å^2)	σ^2_{calc}(80 K) (10^{-4} Å^2)	σ^2_{calc}(300 K) (10^{-4} Å^2)
200	474±10	11.7±0.5	11.7	22.9	34.6
250	475±10	11.6±0.5	11.6	22.8	34.4
300	473±10	11.8±0.5	11.8	22.9	34.8
350	469±10	12.1±0.5	12.1	23.2	35.3
400	471±10	11.9±0.5	11.9	23.1	35.0
650	470±10	12.0±0.5	12.0	23.1	35.1
800	474±10	11.7±0.5	11.7	22.9	34.6

which causes changes in the atomic position of As neighbors.

Below the melting temperature, the value of relative structural disorder is significantly decreased with increasing annealing temperature. As a function of T_Q, $\Delta\sigma^2$ shows a deep minimum at 300 °C, a temperature slightly less than the melting temperature. The decrease in $\Delta\sigma^2$ between T_Q and T_M in Fig. 5 indicates a strong tendency toward ordering. This 300 °C annealed sample represents the lowest-free-energy metastable g state.

Monoclinic orpiment has a layered structure[28] in which the molecular unit, AsS_3, is macroscopically extended in two dimensions with layers stacked along the b axis. Within the layers, each As atom is bonded to three S atoms in a triangular pyramidal arrangement with an As atom at apex and three S atoms at the bases. The ratio between interlayer to intralayer bond length of ~ 1.57 indicates that the adjacent layers are held together principally by weak van der Waals forces so that there is perfect cleavage normal to the [010] direction. In each layer, the atoms are arranged in the order S-As-S-As as helical chains running parallel to the c axis. Within the unit cell there are two inequivalent S sites. The AsS_3 pyramidal units are linked together in the helical chain at the first S site and the helices are joined at the second bridging S site. The bond angle As—S—As of the bridging S site is 14% smaller than the corresponding bond in the chain. The longest of the six As—S bond distances is that between an As and a bridging S atom. Because the average first neighbor distances of c- and g-As_2S_3 are the same, the structural disorder effect is confined to small changes of bond angle between molecular units. Contributions to the structural disorder in g-As_2S_3 can be conveniently divided into two categories: (1) distortions in the As—S—As bond angle, i.e., the S bridge between or along helices and the S atom within a helix, and (2) deviations in the As apex angles.

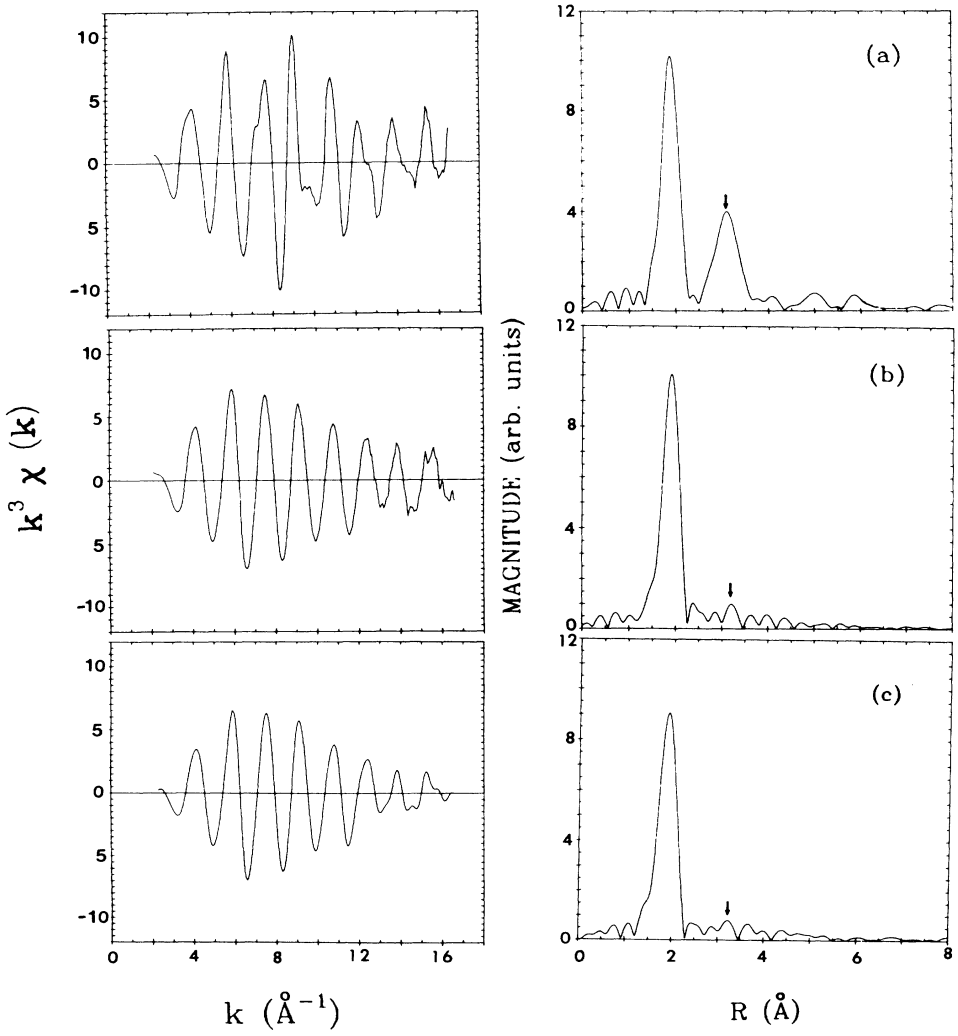

FIG. 4. $k^3\chi(k)$ spectra and corresponding Fourier transforms for (a) c-As_2S_3, (b) g-As_2S_3 quenched at 300 °C, and (c) g-As_2S_3 quenched at 800 °C.

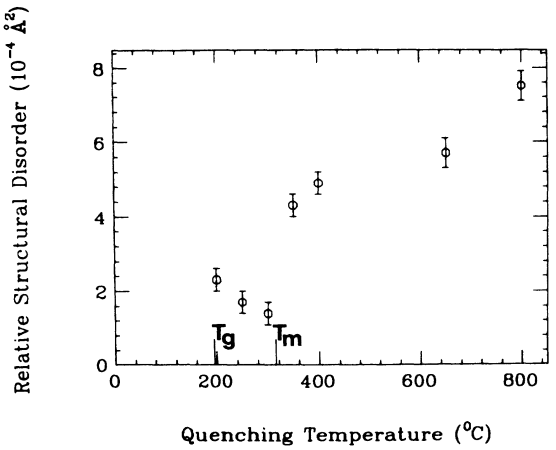

FIG. 5. Value of relative structural disorder $\Delta\sigma^2$ quenching temperature T_Q for g-As_2S_3 samples.

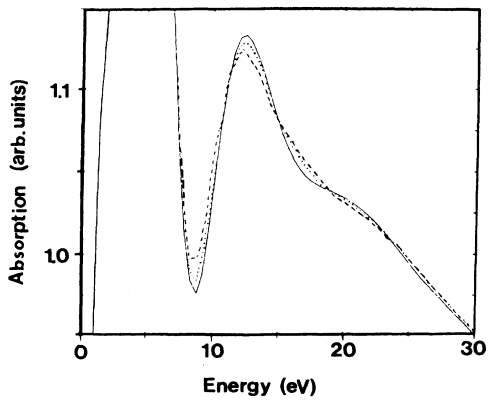

FIG. 6. Expanded view of the XANES spectra. Solid line, c-As_2S_3; dotted line, g-As_2S_3 quenched at 300 °C; dashed line, g-As_2S_3 quenched at 800 °C.

Topologically, the structural distortions of As—S—As angles are easily achieved. The bond geometry of twofold coordinate S atoms is relatively unrestricted; furthermore, for the bridging S atoms a weak binding force exists because of the longer bond distance. Because of this As—S—As bond angle freedom there is a manifold of allowed structural orientations. In the absence of a good standard compound and because of the larger disorder of the glass samples due to structural and thermal disorder, the second main coordination shell of these samples is difficult to analyze in detail so that a simple approximation may be made to calculate the bond-angle deviation $\Delta\Theta$. The second peak of Fourier transform shown in Fig. 4 is due to contributions from the As-As distance in a S-As-S-As helix and interchain As-S-As linkages as in c-As_2S_3. If we accept the x-ray diffraction results,[7] the second coordination number and As—As bond distance of g-As_2S_3 are the same as for c-As_2S_3. A relatively small change of the As—S—As bond angles will cause a $\Delta\sigma^2$ in the second shell. The relationship between $\Delta\sigma^2$ and $\Delta\Theta$ in the second shell can be written as[29]

$$\Delta\sigma^2=[r_1\cos(\tfrac{1}{2}\Theta_0)\Delta\Theta]^2 . \quad (8)$$

We find that the distribution of As—S—As bond angles has a root-mean-square distortion $\Delta\Theta$, which is 3° smaller for the sample quenched at 300 °C than for the sample quenched at 800 °C, using $R_{\text{As-S}}=2.28$ Å and $\Theta_0=100°$ with As-As amplitude and phase determined from the second shell of c-As. This also explains one of the reasons the adjacent As atoms are distorted from their crystalline positions. Other contributions to $\Delta\sigma^2$ come from the deviation in the S—As—S pyramid apex angles. Our experimental results[30] on laboratory synthesized orpiment from bulk glasses confirmed the above suggestion. It was proposed by Smith *et al.*[31] that the helical chains of alternating As and S atoms, which occur parallel to the c axis, provide a built-in growth spiral in the classical pattern of the crystal-growth mechanism. Hence, the structural relaxation process leading towards a more-ordered glassy state involves, to some extent, the reorientation of the As apex angles. This implication is supported by the nuclear quadrupole resonance data of Rubinstein and Taylor,[32] who found that the As apex angle of g-As_2S_3 deviates about 2° from that of c-As_2S_3.

The XANES is sensitive to the geometrical arrangement of the environment surround the absorbing atom, but a detailed analysis of this part of XAS spectra is more difficult since it involves theoretical calculations to account for multiple scattering effects.[18] At this time only qualitative comparisons are discussed. The main large absorption peak, "white line," in Fig. 1 is similar in all spectra. The white line in the As K edge corresponds to the transition from a $1s$ core state to a final unfilled $4p$ state associated with the antibonding sp^3 states. About 10 eV above the white line, the spectra look different. An expanded view of the XANES region for the data of c- and g-As_2S_3 samples quenched at 300 and 800 °C is compared in Fig. 6. The changes in the second feature occur between g-As_2S_3 samples. These changes are associated with the trend toward the ordered state. This is consistent with EXAFS analysis which found that the sample quenched at 300 °C is in the well-relaxed, more-ordered state. A more-detailed analysis of these changes associated with quenching and composition effects is currently underway.

Our results on g-As_2S_3 indicate the presence of structural order beyond a single AsS_3 pyramid. Because of large structural and thermal disorder in the higher shells, with the EXAFS technique it is difficult to infer the existence of chains or layer segements. At the present stage, with EXAFS it is not possible to confirm whether interlayers become smoother with increasing temperature above T_Q, as proposed by Busse[3] from x-ray diffraction results. However, her suggestion of decreased structural order within each layer associated with the second x-ray diffraction peak is ruled out. The decreasing intensity in the second diffraction peak with increas-

ing temperature may be expected due to thermal contributions rather than structural disroder in the Debye-Waller factor. The model suggested by Kawamura *et al.*[13,14] from low-frequency Raman scattering results is also ruled out. Their model, in which structural relaxation will never occur for the sample quenched at 300 °C, is contradicted by our results. Although our EXAFS results alone do not make it possible to develop an intermediate-range order (IRO) model of g-As_2S_3, it is possible to rule out some suggested IRO models by correlating EXAFS measurements with other experiments.

Our studies show that measurement of the structural disorder in EXAFS can yield important information about how much local configurations of materials may differ due to different preparation or other treatments on the same sample. In particular, EXAFS studies can be useful in studying ordering in some glassy systems which have been difficult to crystallize in the laboratory. For example, it has long been assumed that there were kinetic barriers to the formation of c-As_2S_3. Using the EXAFS technique, we discovered a method[30] for producing c-As_2S_3 and determining a tendency for ordering manifested in the relative structural disorder factor for a specific recipe. Preliminary studies on g-As_2Se_3 and g-As_4Se_4 also show specific temperature ranges where ordering occurs and initial annealing studies show that crystallization may be occurring.

Considering the thermal quenching rate on the structure of g-As_2S_3, the following conclusions are made: The structure of g-As_2S_3 does not undergo significant changes at quenching temperatures between 350 and 800 °C. The trend toward a more-ordered structure is observed at quenching temperatures between 200 and 300 °C. Based on the above results, we identified the g-As_2S_3 samples quenched at 300 °C as the well-relaxed state among all g-As_2S_3 samples we studied. Structural changes in terms of modification of the g-As_2S_3 structure are due to two factors: distortions of the As—S—As bond angles and deviations of the As apex angles.

ACKNOWLEDGMENTS

The authors would like to thank Dr. Y. Y. Chu of Brookhaven National Laboratory for help in sample preparation. One of us (C.Y.Y.) is also pleased to acknowledge informative discussions with Dr. S. M. Heald. This work is supported by the Department of Energy under Contract No. DE-AS05-80ER10742 and the National Science Foundation under Grant No. DMR-84-07265.

[1]N. F. Mott and E. A. Davis, *Electronic Properties in Non-Crystalline Materials,* 2nd ed. (Clarendon, Oxford, 1979), and references therein.
[2]K. Tanaka, J. Non-Cryst. Solids **35/36**, 1023 (1980).
[3]L. E. Busse, Phys. Rev. B **29**, 3639 (1984).
[4]R. A. Street, T. M. Searle, I. G. Austin, and R. S. Sussmann, J. Phys. C **7**, 1582 (1974).
[5]F. Kosek, Z. Cimpi, J. Ttulka, and M. Matyas, in *Structure and Properties of Non-Crystalline Solids,* edited by B. T. Kolomiets (Academie of Science of the USSR, Leningrad, 1976), p. 331.
[6]C. Y. Yang, D. E. Sayers, and M. A. Paesler, *National Synchrotron Light Source Annual Report* (Brookhaven National Laboratory, New York, 1985), p. 203.
[7]A. A. Vaipolin and E. A. Porai-Koshits, Fiz. Tverd. Tela. (Leningrad) **5**, 246 (1963); **5**, 256 (1963); 5, 683 (1963) [Sov. Phys.—Solid State **5**, 178 (1963); **5**, 186 (1963); **5**, 497 (1963)].
[8]S. Tsuchihashi and Y. Kawamoto, J. Non-Cryst. Solids **5**, 286 (1971).
[9]A. J. Leadbetter and A. J. Apling, J. Non-Cryst. Solids **15**, 250 (1974).
[10]A. C. Wright and A. J. Leadbetter, Phys. Chem. Glasses **17**, 122 (1976).
[11]A. I. Sokalakov and V. V. Nechaeva, Fiz. Tverd. Tela. (Leningrad) **9**, 921 (1967) [Sov. Phys.—Solid State **9**, 715 (1967)].
[12]A. C. Wright, R. N. Sinclair, and A. J. Leadbetter, J. Non-Cryst. Solids **71**, 295 (1985).
[13]H. Kawamura, T. Takasuka, T. Minato, T. Hyodo, and T. Okumura, J. Non-Cryst. Solids **59/60**, 863 (1983).
[14]H. Kawamura, F. Fukumasu, and Y. Hamada, Solid State Commun. **43**, 229 (1982).
[15]J. C. Phillips, J. Non-Cryst. Solids **43**, 37 (1981).
[16]R. J. Nemanich, J. Non-Cryst. Solids **59/60**, 851 (1983).
[17]R. J. Nemanich, Phys. Rev. B **16**, 1655 (1977).
[18]*X-ray Absorption Principles, Applications, Techniques of EXAFS, SEXAFS and XANES,* edited by D. Koningsberger and R. Prins (Wiley, New York, in press), and references therein.
[19]E. A. Stern and K. Kim, Phys. Rev. B **23**, 3781 (1981).
[20]E. A. Stern, Phys. Rev. B **10**, 3027 (1974).
[21]D. E. Sayers, F. W. Lyttle, and E. A. Stern, Phys. Rev. B **11**, 4836 (1975).
[22]E. Sevillano, H. Meuth, and J. J. Rehr, Phys. Rev. B **20**, 4908 (1979).
[23]B. A. Bunker, Ph.D. thesis, University of Washington, 1980 (unpublished).
[24]C. Y. Yang, M. A. Paesler, and D. E. Sayers, J. Phys. (Paris) Colloq. **47**, C8-391 (1986).
[25]C. Y. Yang, M. A. Paesler, and D. E. Sayers, Phys. Rev. B **36**, 980 (1987).
[26]M. B. Myers and E. J. Felty, Mater. Res. Bull. **2**, 535 (1967).
[27]K. Tanaka, S. Gohda, and A. Odajima, Solid State Commun. **56**, 899 (1985).
[28]D. J. E. Muller and W. Nowacki, Z. Kristallogr. **136**, 48 (1972).
[29]M. A. Paesler, D. E. Sayers, R. Tsu, and J. G. Hernanadez, Phys. Rev. B **28**, 4550 (1983).
[30]C. Y. Yang, M. A. Paesler, and D. E. Sayers, Materials Lett. **4**, 233 (1986).
[31]B. A. Smith, N. Cowlan, and A. M. Shamah, Philos. Mag. B **39**, 111 (1976).
[32]M. Rubinstein and P. C. Taylor, Phys. Rev. B **9**, 4258 (1974).